

Corrosion monitoring by optical inspection with coherent and incoherent light

V. NASCOV*, C. SAMOILĂ, D. URSUȚIU
Transylvania University of Braşov, Romania

An experimental study on corrosion monitoring by using optical methods, in both coherent and incoherent light is presented. The corrosion is a surface degradation process and the optical methods, especially that based on coherent light, are sensitive techniques to detect surface alterations. A metal or alloy sample is introduced into a corrosion cell connected to a PGstat device. While the sample undergoes a corrosion process at a rate controlled by the PGstat device, its surface is illuminated incoherently and inspected periodically by a digital microscope. Then, another setup is used: the sample is illuminated by coherent light and a video camera without lens records speckle patterns in an objective speckle setup. The two techniques are compared and it is pointed out what new information is revealed in the case of coherent illumination.

(Received February 5, 2014; accepted November 13, 2014)

Keywords: Corrosion monitoring, Electrochemistry, Dynamic speckle

1. Introduction

Corrosion is generally an undesired degradation process of materials and it often should be measured, monitored and predicted in order to reduce some economical losses. The conventional methods widely used to measure corrosion are the electrochemical methods [1]. A metal gets corroded if it loses electrons as a result of electrochemical interactions with other substances. While losing electrons, it also loses a proportional number of its constitutive atoms, transformed in positive ions, no more supported by the metallic structure. Measuring the current of electrons that leave the metallic structure, i.e. the corrosion current, forms the basis of measuring the corrosion rate, which is proportional to the corrosion current. However, the corrosion current cannot be measured directly because the electronic current is cancelled out by the ionic current, in the case of normal, spontaneous corrosion at equilibrium. There are only indirect electrochemical methods to measure the corrosion current. A sample of the investigated material is usually put in a three-electrodes corrosion cell and these methods apply electrical perturbations to record the electrical response of the corroding system [2, 3]. In order to determine the corrosion current one needs to apply a very large cell current compared to the actual corrosion current (dc voltammetry and Tafel analysis) and the measuring process itself may lead to surface alterations (accelerated, stimulated corrosion) that falsify the results. A class of methods applies just small perturbations to the corroding system (small amplitude voltammetry) and measure the polarization resistance, which is proportional to the corrosion current [3]. This enables to monitor the variations of the corrosion activity, but the effective corrosion rate remains undetermined, because some other

required electrical parameters (anodic and cathodic coefficients) cannot be accurately measured by this class of methods.

Moreover, corrosion is a complex process that depends on many factors: the initial surface conditions, as well as the environment conditions. Corrosion occurs generally neither uniform over the surface, nor constant over time. An average corrosion rate can be measured by microgravimetric methods over a very long time. Alternative methods are needed for shorter term measurements.

Optical methods for corrosion monitoring are not unknown, but quite rarely used. There are methods based on incoherent light, such as simple surface inspection by microscopy [4, 5] and methods based on coherent light such as interferometry, holography and speckle methods. Interferometry and holography are able to detect punctually the surface alterations with very high sensitivity, but are impractical for in-situ corrosion monitoring. Despite of this, there are some papers about holographic techniques for corrosion monitoring [6, 7]. The speckle methods are very robust, very simple and can provide measurements in terms of statistical properties of the surface [8-11]. This paper is concerned with the last category of speckle methods. A common fact of most optical methods up to now documented is that they give rather qualitative than quantitative characterization of the corrosion process.

Speckle methods are commonly used to investigate the statistics of surface processes. Due to the surface activity (corrosion process), the speckle pattern has a dynamical evolution. There are well established methods to deal with dynamic speckle [8-10]. In our study we track some statistical quantities of the speckle pattern and try to find those that seem to be best correlated to the corrosion

process. Next we describe the used procedures and the steps we have followed looking for meaningful results.

We have used samples made of copper, some copper alloys, steel and stainless steel and we studied their corrosion behaviour in seawater.

2. Investigations with incoherent light

We have built up a setup designed to study corrosion, which consists of a special corrosion cell that supports a digital microscope to inspect the sample surface while it undergoes corrosion.

The sample has the shape of a 15mm diameter disk and is hold by a special designed electrodes support, sketched in Fig. 1. This support holds a reference electrode too, which don't need a Luggin capillary, as commonly used in electrochemistry.

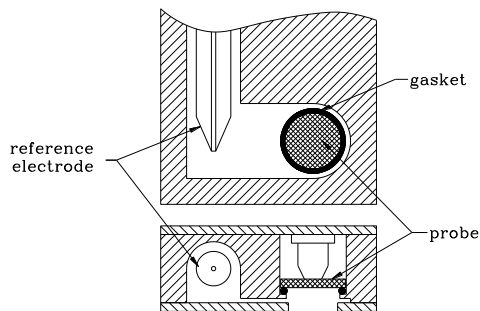


Fig. 1. The electrodes support of the corrosion cell.

The corrosion cell is transparent and is filled up with the electrolyte (seawater). It is connected to a PGstat apparatus and a computer is used to drive the devices and to process the data. The setup is described in paper [5].

By adding a contraelectrode the cell becomes a standard three-electrode cell as used for corrosion measurements by electrochemical methods. This enables to conduct at the same time electrochemical and optical methods.

A series of metal and alloy samples were investigated. They were illuminated by a couple of white LEDs. At the time of publishing [5] we made simple observations of the surface alterations during electrochemical measurements or controlled electrochemical processes.

Now, in order to get an objective analysis we track the following physical quantities regarding to the images acquired by the microscope, for each of the R,G,B channel:

-the average brightness:

$$\langle I \rangle_{(R,G,B)} = \frac{1}{N_x N_y} \cdot \sum_m \sum_n^{N_x N_y} I_{mn}(R,G,B),$$

-the standard deviation of the brightness:

$$\sigma_{I(R,G,B)} = \sqrt{\left\langle \left(I_{(R,G,B)} - \langle I \rangle_{(R,G,B)} \right)^2 \right\rangle},$$

$$\text{-the contrast: } V_{(R,G,B)} = \frac{\sigma_{I(R,G,B)}}{\langle I \rangle_{(R,G,B)}}$$

where N_x and N_y are the pixel resolutions along horizontal and vertical direction of a rectangular window cropped from the image. The average brightness shows how the reflectivity of the sample surface evolves as a consequence of corrosion or other electrode processes. The contrast variations indicate the localization degree of the surface processes.

We have tracked these quantities during a so called reversibility test: the PGstat is set to record a series of cyclic voltammograms with different scan rates, in a quadratic progression: 9, 16, 25, 36, 49, 64, 81, 100 mV/s. There are occurring anodic and cathodic processes on the sample surface during each cycle. If these processes are electrochemically reversible, the anodic and cathodic peak currents of that cycles should be in a linear progression, as stated by a law of Cottrell [1]. By setting appropriate scan limits, we have got this condition satisfactory fulfilled in the case of a copper sample in seawater, as shown in Fig. 2.

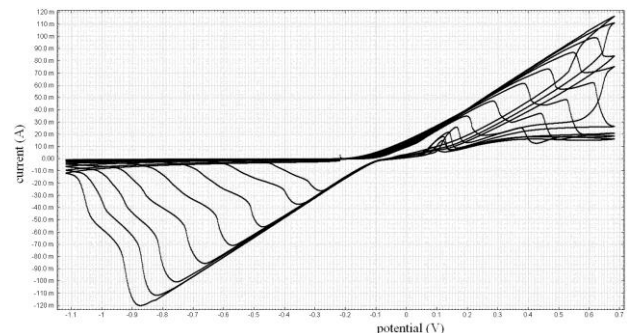


Fig. 2. A set of cyclic voltammograms recorded with different scan rates, in a quadratic progression.

How the optical response of the sample is related to this reversibility test is shown in the graphs below: the evolution of the average brightness during all these voltammetric cycles is plotted in Fig. 3 and the contrast evolution is plotted in figure 4. The images were acquired at a rate of one frame/s. Before starting this test the sample is left at its open circuit potential for 200 s and the initial surface reflectivity is high. Right after starting the first voltammetric cycle the reflectivity decreases sharply, but exhibits quite reversible variations over the next cycles. The surface processes are not uniform, as indicated by the contrast variations. However, the average contrast is relative constant over the voltammetric cycles.

So far, by using these methods we could not get more than a qualitative analysis of the corrosion processes.

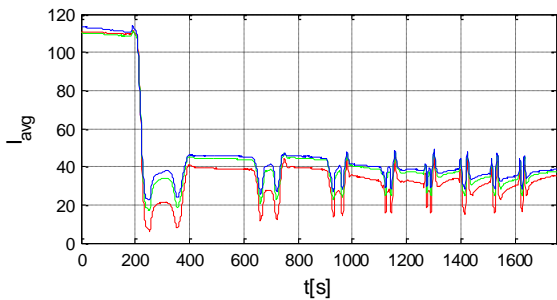


Fig. 3. Evolution of the RGB average brightness during the reversibility test (on a scale from 0 to 255 units).

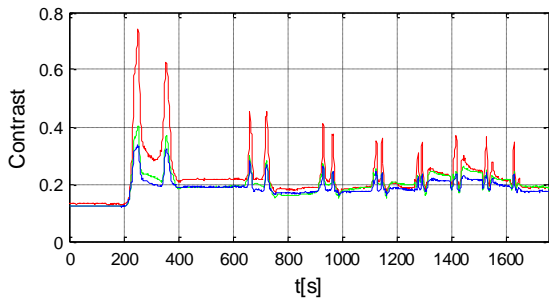


Fig. 4. Evolution of the RGB contrast during the reversibility test.

3. Investigations with coherent light

3.1 Experimental setup

We have built up an experimental setup as that sketched in Fig. 5. This is a setup for objective speckle. In our first experiments we used the same corrosion cell as in the case of incoherent illumination. The sample is now illuminated by a frequency-doubled solid state laser pumped by a laser diode, with a stabilization unit that enables power adjusting. The output light is green ($\lambda=532\text{nm}$), but the beam contains also the strong IR pumping ray. This is the reason why we use the IR cut-off filter. The sample is hit by a laser spot smaller than 1mm.

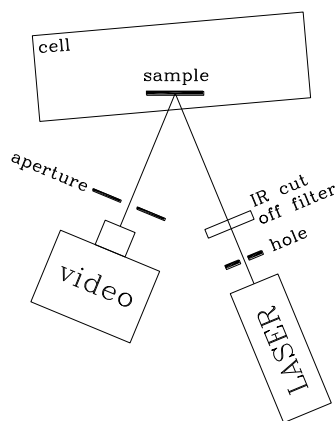


Fig. 5. Experimental setup.

The video camera is a low cost old VGA CMOS webcam with the objective removed. It records the scattered light which builds up an objective speckle pattern on the CMOS area, smaller than 4×3 mm, with the resolution of 640×480 pixels.

Firstly, we carried out pure optical experiments, leaving the sample alone in the solution, to undergo spontaneous corrosion, for a time while a series of speckle patterns are acquired.

The image acquisition is coordinated by a PC through a NI LabVIEW application, using the additional NI Vision Builder package, which offers a driver for the video camera.

The appearance of the speckle pattern depends on the sample roughness. If the surface is very smooth (small rms roughness compared to the wavelength) the speckle pattern is partially developed, as seen in Fig. 6a. The scattered light contains a specular component and a diffuse component. We get such a speckle pattern by carefully sanding the sample with #2000 grit paper. It is possible to measure the roughness by analyzing the specular and diffuse components. However, we didn't use this possibility in the present study, because the video camera should be well centered on the specular direction (equal incidence and reflection angles) and the above mentioned IR ray is so strong along this direction, that it generates a strong parasitic speckle pattern. The IR cut-off filter cannot filter it completely.

If the roughness is coarse enough (rms roughness well greater than the wavelength), the specular component disappears and the speckle pattern looks like that shown in Fig. 6b. This is a fully developed speckle pattern and its appearance is no longer dependent on the further increase of roughness or on the surface statistics. We obtain such a speckle pattern by sanding the sample with #500 or coarser grit paper. This is the speckle case we used so far in our study. We usually set the recording direction close to the specular direction.

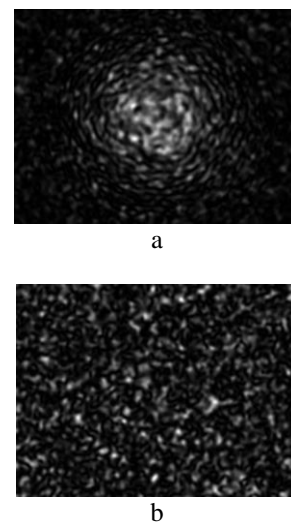


Fig. 6. Simulated objective speckle patterns; a) partially developed speckle pattern, b) fully developed speckle pattern.

The sample is placed near the wall of the cell (4-5mm) in order to keep the way of light through the liquid as short as possible, to minimize scattering on liquid impurities. The sample surface should be a bit wedged in respect to the cell wall, in order to send away the reflections of light on the wall faces, which generate a system of Young fringes. The aperture in front of the camera (5mm large) helps to block some parasitic reflections.

We get fringe patterns as that shown in Fig. 7a. In our experiments we set the image acquisition rate to 1 frame/s. The corrosion is a slow process, but there is noise coming from other sources and it should be reduced. For this purpose we have used two digital filtering procedures of comparable performance: a moving average filter and a single-pole infinite impulse response filter (IIR).

The moving average filter averages a number of the last images; let us denote this number by N_f . The roll-off frequency of this filter is $\nu_0 = \frac{\nu_s}{\pi N_f}$, where ν_s is the image acquisition rate. We have found that $N_f=50$ last images is a good value to be used, the roll-off frequency being 6mHz (Fig. 7b). Alternatively, we have used an IIR filter with the same roll-off frequency.

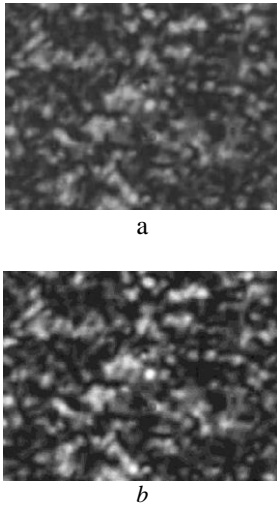


Fig. 7. Real speckle patterns; a) raw image, b) filtered image by averaging the last 50 images.

The statistical quantities that we monitor are computed from the filtered images at an appropriate sampling rate. A sampling rate of twice the roll-off frequency (Nyquist criterion) means one sample every 83s. We have computed one set of statistical quantities every 30s, i.e. twice per minute we used a filtered image to compute the set of statistical quantities.

3.2. Methods and results

We started our study by monitoring the following statistical quantities related to the speckle patterns:

-the average brightness: $\langle I \rangle = \frac{1}{N_x N_y} \cdot \sum_m \sum_n I_{mn}$

-the standard deviation of the average brightness:

$$\sigma_I = \sqrt{\langle (I - \langle I \rangle)^2 \rangle}$$

-the speckle contrast: $V = \frac{\sigma_I}{\langle I \rangle}$

where N_x and N_y are the pixel resolution of the image along horizontal and vertical direction respectively.

In the case of an ordinary steel sample (E295 according to SR EN 10025) immersed in 1M/l seawater, the speckle contrast evolution over 3 hours is shown in Fig. 8. It decreases by more than 30%.

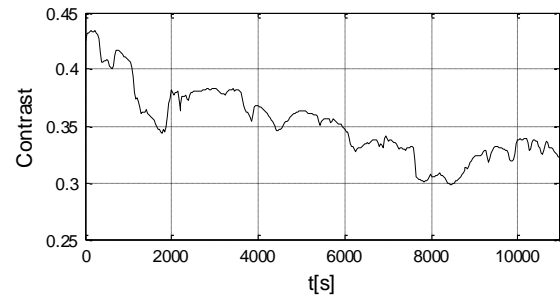


Fig. 8. The speckle contrast evolution in the case of an ordinary steel sample.

If the sample is stainless steel (X 2 CrNi 19 11) the speckle contrast changes slightly (about 5%), as presented in Fig. 9. Note that theoretically, the contrast of a fully developed speckle, assuming Gaussian statistic of the surface roughness should equals 1.

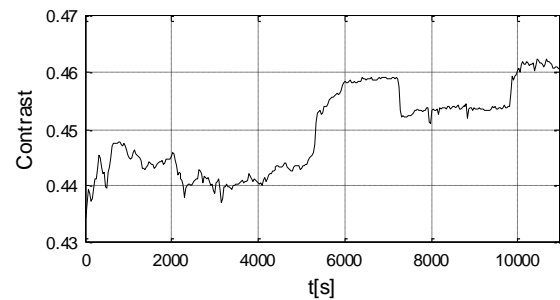


Fig. 9. The speckle contrast evolution in the case of a stainless steel sample.

These results can characterize corrosion in a qualitative way. Another procedure proposed for dynamic speckle is to track a quantity called inter-image distance:

$d_{ij} = \langle (I^{(i)} - I^{(j)})^2 \rangle$, as presented in [9]. This is the mean squared difference of two images indexed by i and j respectively. The pixel intensities of the images are

supposed to be normalized in the range of [0, 1]. We have tracked this quantity for the ordinary steel sample and have got the evolution shown in Fig. 10. The inter-image distance was calculated between the first and the subsequent images.

The curve increases, then it stagnates. The authors of [9] use this procedure to monitor the drying of paints. Their dynamic speckle has a very rapid evolution because, until the paints dry, the pigments move randomly in a Brownian motion. They fitted the curve with the function $d(t) = d_{\max}(1 - e^{-t/\tau})$, where d_{\max} is the stagnation value and τ is a characteristic time of the process. The inverse of τ was called by that authors speckle rate, $SR=1/\tau$. This quantity indicates how fast the speckle evolves.

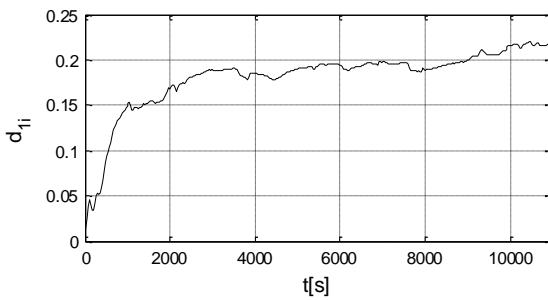


Fig. 10. The inter-image distance evolution of the ordinary steel sample.

We can use the same procedure for corrosion monitoring, but let's see the inter-image distance evolution in the case of stainless steel (Fig. 11). It exhibits an unexpected variation.

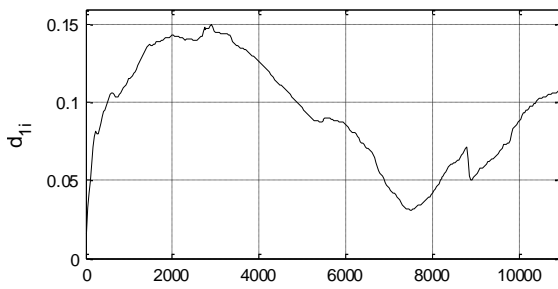


Fig. 11. The inter-image distance evolution of the stainless steel sample.

As we found out later by means of speckle correlation, the sample has moved a bit during the measurements. For the next experiments we fixed better the components in the setup, but small movements are still recorded, because most pieces in the setup are made of plastics.

Therefore, the procedure of inter-image distance tracking is applicable only when providing a very well stability of the setup.

The next technique we have used is the digital speckle correlation [10,11]. The correlation of two speckle patterns indexed by i, j is defined as:

$$C_{ij} = \frac{\langle (I^{(i)} - \langle I^{(i)} \rangle) \cdot (I^{(j)} - \langle I^{(j)} \rangle) \rangle}{\langle (I^{(i)} - \langle I^{(i)} \rangle) \rangle \cdot \langle (I^{(j)} - \langle I^{(j)} \rangle) \rangle} \quad (1)$$

The correlation of two images can be calculated as a function of a translation displacement between those images. There is a certain displacement where the correlation function reaches its maximum. By finding the position of this maximum one can determine the displacement between two similar speckle patterns if the sample has translated between the records. If the sample surface gets altered, the maximum of the correlation function decreases. This is called speckle decorrelation and it is a widely used technique for surface investigation. Its great advantage is that it can separate the surface alterations (microstructure modifications) from the coordinated motions (displacements).

The mean speckle size can be determined as the width of the autocorrelation function (the correlation of a speckle pattern with itself). The (1) formula of the correlation function can be efficiently evaluated by using the Wiener-Khinchin theorem. This implies applying three fast Fourier transforms (FFTs). If using regular fast Fourier transforms for this calculation (as commonly known), we get the autocorrelation function with a very narrow peak, as seen in Fig. 12a. Hence the position and the width of the central peak can be evaluated, but very inaccurately.

We have found a scaled version of the Wiener-Khinchin theorem, which enables zooming into the autocorrelation function [12]:

$$C[I^{(i)}, I^{(j)}] = \text{FFT}^{(-\alpha)}[\text{FFT}^{(-1)}[I^{(i)}] \cdot \text{FFT}^{(1)}[I^{(j)}]] \quad (2)$$

where α is a scale parameter less than one and $\text{FFT}^{(\alpha)}$ denotes the scaled fast Fourier transform. Using this procedure, we get a detailed insight of the central peak of the (auto)correlation function, as seen in Fig. 12b.

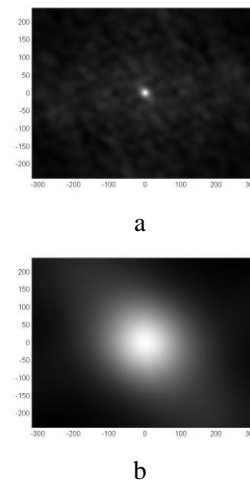


Fig. 12. Correlation function of two speckle patterns; a) computed with regular FFTs, b) Scaled correlation function, enabling more precision to determine speckle displacement and mean speckle size.

Using the scaled correlation between the first and the subsequent images we have determined the translation of the speckle pattern during the three hours of monitoring. Fig. 13 shows the y component of the displacement (the x component was smaller) for the stainless steel sample.

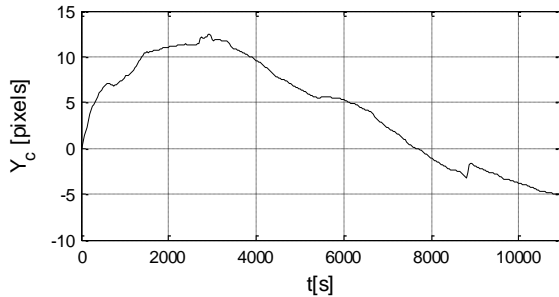


Fig. 13. The speckle translation along y direction in the case of the stainless steel sample.

On the further experiments, after we fixed better the components in the setup, we measured speckle pattern movements of up to 3-4 pixels.

By performing the scaled autocorrelation on each of the filtered images we have determined the mean speckle size, plotted in Fig. 14.

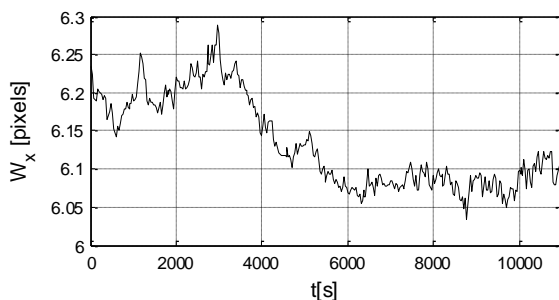


Fig. 14. The mean speckle size along x direction for the speckle patterns of the stainless steel sample.

We also track the speckle decorrelation. The results for ordinary steel and stainless steel are plotted in Fig. 15 and 16 respectively. So far the evolution of this quantity (the maximum of the correlation function) shows the best distinction between the corrosion behaviours of the two different samples.

Up to now we have presented results related to spontaneous corrosion at an unknown, uncontrolled rate (the sample was the single electrode in the cell). The next step in our study was to check all these procedures if the corrosion rate is controlled.

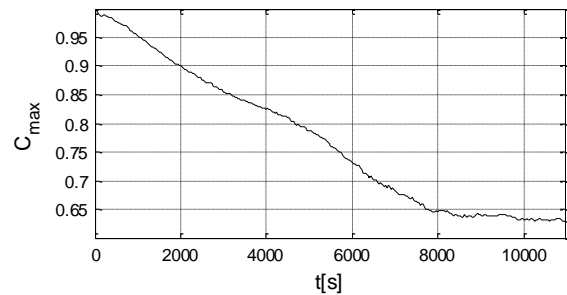


Fig. 15. Speckle decorrelation in the case of the ordinary steel sample.

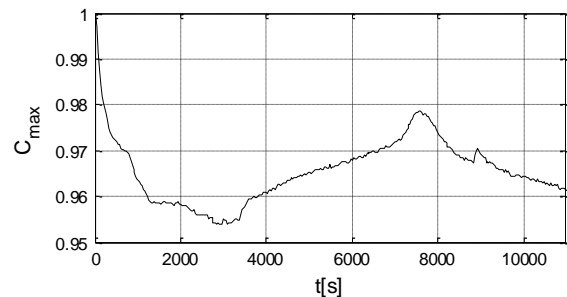


Fig. 16. Speckle decorrelation in the case of the stainless steel sample.

We added a platinum contraelectrode to the cell and made a connection to the sample electrode through a $1M\Omega$ potentiometer. This is the simplest way to establish an adjustable cell current that stimulates the corrosion of the sample. The open circuit voltage of this electrochemical cell was of about 0.6-0.8V.

We repeated the measurements described earlier, by using the same disk electrode, with the following steps:

- spontaneous corrosion for 1800s (zero cell current)
- stimulated corrosion with $33\mu A$ cell current for the next 1800s,
- $66\mu A$ cell current for the next 1800s
- $100\mu A$ cell current for the next 1800s

During this experiment the cell current needed occasionally minor manual adjustments.

We expected to find out that the corrosion cell current greatly influences the evolution of all tracked statistical quantities of the speckle in a manner that would lead to a quantitative relationship between the corrosion rate and some of the optically measured quantities. Surprisingly, we could not find any covariance between the cell current and any of the tracked statistical quantities. A greater cell current did not always cause a faster decorrelation or decrease of the speckle contrast. Therefore, we concluded that the sample electrode should be redesigned. The former sample has a very large area compared to the very small laser spot size. If the corrosion takes place not uniformly over the sample area, the investigated area (illuminated by the spot) cannot provide information about the average corrosion rate.

The newly designed sample electrode has the shape of a truncated cone as sketched in Fig. 17. It is coated by

black pigmented epoxy resin, excepting the front surface, which is polished and this is the only one corrosion active area, exposed both to the electrolyte and the laser beam. It is a bit smaller than the laser spot (0.7mm diameter), so that the whole active area gets illuminated and the part of light that does not fall onto this area goes away and does not contribute to the speckle pattern.

We repeated the last experiment using the new sample electrode made of ordinary steel:

- spontaneous corrosion for 1800s (zero cell current)
- stimulated corrosion with $1\mu\text{A}$ cell current for the next 1800s,
- $2\mu\text{A}$ cell current for the next 1800s
- $4\mu\text{A}$ cell current for the next 1800s

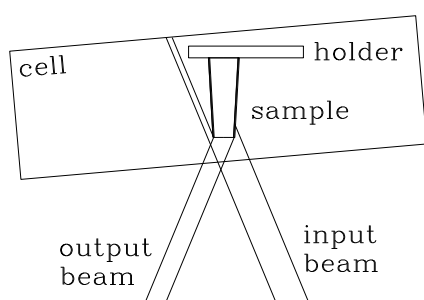


Fig. 17. A new sample electrode.

Now we get data that show clearly the influence of the cell current on the decorrelation rate (as well as other quantities). In the Fig. 18 are plotted together the decorrelation curves for each of the four time intervals. The upper curve is the correlation between the first image and the subsequent ones, up to the moment $t=1800\text{s}$. The next curve is the correlation between the image at the moment $t=1800\text{s}$ and the subsequent ones, up to the moment $t=3600\text{s}$; and so on...

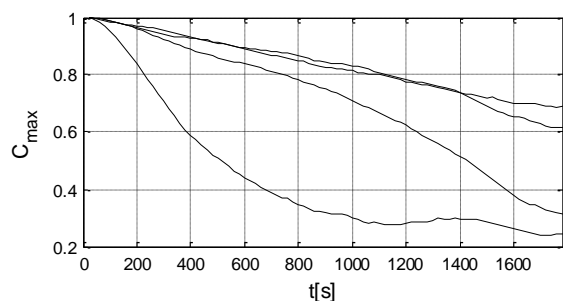


Fig. 18. Speckle decorrelation influenced by the cell current.

The spontaneous corrosion current is unknown, but the decorrelation curve in this case is so close to the decorrelation curve for $1\mu\text{A}$ cell current, that we can think the spontaneous corrosion current is close to $1\mu\text{A}$. A cell current of $1\mu\text{A}$ means a current density of $250\mu\text{A}/\text{cm}^2$ at

this sample surface. The corrosion current density of steel is reported to be of $10\text{-}20\mu\text{A}/\text{cm}^2$ (depending on the steel alloy). Now there is another issue: the corrosion rate is not constant and it depends on the initial surface conditions. We started our measurements right after sanding the probe, and it is highly probably that the surface is very corrosion active on the beginning.

4. Conclusions

We have studied the possible use of optical methods to characterize corrosion, both with incoherent light (microscopy) and coherent light (speckle techniques). The microscopy allows simple observations of the sample surface and a pure qualitative characterization of the surface processes by tracking the overall reflectivity and contrast.

The investigations with coherent light offer the best chances to find quantitative results, in terms of statistical quantities. The best indicator of the corrosion proved to be the speckle correlation tracking, close related to the average change of the surface height profile. We confronted with two major issues:

1. The corrosion is generally not uniform and the laser spot should illuminate the whole sample area in order to measure the overall (or average) corrosion rate.
2. The corrosion rate is not constant. There is no accurate method to measure it at any given moment and it is difficult to assess an optical method without a suitable reference method.

Once we will be able to demonstrate a valid quantitative relationship between the corrosion rate and one optically measured quantity (this being the main objective of our research), the initial setup that uses a large sample illuminated by a small spot will be usable to measure the corrosion locally.

Acknowledgements

This paper is supported by the Sectorial Operational Programme Human Resources Development (SOP HRD), financed from the European Social Fund and by the Romanian Government under the contract number POSDRU/88/1.5/S/59321.

Many thanks to Mr. Dr. Mircea Udrea, who provided us with the well stabilized laser needed to carry out the experiments.

References

- [1] V. S. Bagotsky, "Fundamentals of electrochemistry", © John Wiley & Sons (2001).
- [2] T. Hemmingsen, H. Lima, *Electrochimica Acta*, **43**(1-2), 35 (1998).
- [3] F. Mansfeld, *J Solid State Electrochem*, **13**, 515 (2009).
- [4] T. Hemmingsen, F. Fusek, E. Skavås, *Electrochimica*

- Acta, **51**(14), 2919(2006).
- [5] V. Nascov, D. Ursuțiu, C. Samoilă, Proc. of the 8th Int. Conf. on International Conference on Remote Engineering and Virtual Instrumentation - REV' 2011, Brasov, Romania ISBN 978-3-89958-555-1.
- [6] K. Habib, K. Bouresli, ELECTR ACT, **44**(25), 4635 (1999).
- [7] K. Habib, K. Bouresli, Nondestructive Testing and Evaluation, **15**(2), 1477 (1999).
- [8] M. Vannoni, M. Trivi, R. Arizaga, H. Rabal, G. Molesini, Eur. J. Phys. **29**, 967 (2008).
- [9] L. Brunel, A. Brun, P. Snabre, L. Cipelletti, Opt Express **15**(23), 15250 (2007).
- [10] A. Federico, G. H. Kaufmann, Optics Communications **267**, 287 (2006).
- [11] T. Fricke-Begemann, PhD thesis, University of Oldenburg, Germany, (2003).
- [12] V. Nascov, C. Samoilă, D. Ursuțiu, AIP Conference Proceedings, **1564**(1), 217 (2013).

*Corresponding author: victor.nascov@unitbv.ro